Title:

A database of submarine landslides offshore West and Southwest Iberia

Authors:

Davide Gamboa

Instituto Português do Mar e de Atmosfera – IPMA, I.P.; Rua C do Aeroporto, 1749-077 Lisbon, Portugal

davide.gamboa@ipma.pt

Twitter: @GambixPT

Rachid Omira

Instituto D. Luiz – IDL; Faculdade de Ciências da Universidade de Lisboa, Campo Grande, Edifício C8, Piso 3, 1749-016 Lisbon, Portugal

raomira@fc.ul.pt

Pedro Terrinha

Instituto Português do Mar e de Atmosfera – IPMA, I.P.; Rua C do Aeroporto, 1749-077 Lisbon, Portugal

pedro.terrinha@ipma.pt

Corresponding author:

Davide Gamboa – davide.gamboa@ipma.pt

Data Descriptor Template

Title

A database of submarine landslides offshore West and Southwest Iberia

Authors

Davide Gamboa[1], Rachid Omira[1,2], Pedro Terrinha[1,2]

Affiliations

1. Instituto Português do Mar e de Atmosfera – IPMA, I.P.; Rua C do Aeroporto, 1749-077 Lisbon, Portugal
2. Instituto D. Luiz – IDL; Faculdade de Ciências da Universidade de Lisboa, Campo Grande, Edifício C8, Piso 3, 1749-016 Lisbon, Portugal

corresponding author(s): Davide Gamboa (davide.gamboa@ipma.pt)

Abstract

Submarine landslides are major geohazards occurring on distinct seabed domains ranging from shallow coastal areas to the deeper points of the ocean. The nature and relief of the seabed are key factors influencing the location and size of submarine landslides. Efforts have recently been made to compile databases of submarine landslide distribution and morphometry, a crucial task to assess submarine geohazards. The MAGICLAND (Marine Geo-hazards Induced by underwater Landslides in the SW Iberian Margin) database here presented contributed to that assessment offshore Portugal. Based on EMODnet bathymetric DEMs and GIS analysis, the morphometric properties of 1552 submarine landslides were analysed and wealth of 40 parameters was obtained. This dataset is now made available for the free use and benefit of the international marine community. Further contributions or analysis based on, and complementing the MAGICLAND database will be welcome.

Background & Summary

Submarine mass movements are common occurrences on marine domains, from the shallow coasts to the deepest areas of the oceans [1]. The resulting landslides can be characterised by a variety of deposit features and morphologies, influenced by the mechanic properties of the original strata, the dynamics of the flow processes, regional geology and seismicity. Although singular massive deposits attract the attention for detailed studied, the regions where they occur can record geological evidence of hundreds or thousands of smaller-scale landslides, often poorly covered by available data and of limited focus of analysis.

Submarine landslides are a primary geohazard in marine environments. Tsunamis generated from landslides on the flank of subaerial topography flowing into the sea[2], or from large collapses on fully submerged morphologic features [3] are a major concern. Moreover, geotechnical installations and infrastructures resting on the seafloor such submarine communication cables, pipelines or any purpose-build platform are sensible to mass movements[4]. Submarine landslides impact in marine biological communities, either by acting as habitat hotspots on their scars and remobilised elements or by disturbing and modifying seafloor ecology during emplacement [5]. Recognising submarine landslide extents has further political implication as these are used to set international ZEE boundaries under the definition of the UN Convention on Law of the Sea[6]. It is thus crucial to understand the distribution patterns and morphometric trends of submarine landslides according to the regional setting in which they occur, and aim to unravel insights on their causes and deposits[1,7].

Efforts have been made to compile databases of submarine landslides with the aim of better understanding their distribution and characteristics on marine settings around the world[1,7]. Regional compilations are available from the US Atlantic margin[8,9], the Mediterranean Sea[10], the Spanish margins[11] or Australia[12]. Global data compilations have also allowed the comparison of landslides on distinct geological settings[7,13,14]. However, extensive submarine landslide characterisation is still lacking in many continental margins, and adequate characterisation depends on the quality of available data. Such is the case of the West and Southwest Iberian Margin, on the Northeast Atlantic Margin. This is an area of relevant geological risk, with frequent seismic activity resultant from the NW-ward collision of the African and European tectonic plates[15,16]. This has led to the occurrence of several high magnitude earthquakes (Mw>7), from which the 1755 Lisbon Earthquake and tsunami is one of the major natural disasters recorded[17]. Furthermore, the chains of large seamounts that occur in the area create major bathymetric features rising up to five kilometres above from the abyssal plain depths[16] area associated to intermediate to large seismicity, which is known to be a landslide trigger. Instability susceptibility studies conducted on the study area indicate that large extents of the continental slope and seamounts are prone to failure[18,19]. Yet, few submarine landslide studies exist, and these focused on specific case studies[3,20–22].
It is thus crucial and timely to provide a broader perspective of the distribution and morphometric trends of submarine landslides offshore Iberia. This work presents the MAGICLAND (Marine Geo-hazards Induced by underwater Landslides in the SW Iberian Margin) database, which covers the geographical area from 33º45' to 43º N and from 6º22' to 16º 15W, and compiled geomorphological data of 1552 submarine landslides based on the interpretation of DEM bathymetric grids provided by EMODnet[23] (Figure 1). Our results are crucial to understand the broad distribution of geohazards on the area, and aim to contribute to global efforts to compile landslide information in different geological and oceanic settings. This dataset is openly available through the Open Science Framework data repository[24] for the use and benefit of the international marine and geohazard community. Further contributions or analysis based on, and complementing the MAGICLAND database will be welcome.

Methods

This section describes the methodology workflow of the data acquisition and preparation. This was set in three main stages, namely the Digital Elevation Model (DEM) data loading, the mapping of landslide features, and volume calculation procedures. The main steps for each process are summarised in Figure 2.

DEM loading and referencing

The mapping of scars and landslide features was based on DEMs available through the 2018 version of the EMODnet DTM for European seas covering the Southeast Iberian margin[23] (Figure 1). The EMODnet datasets result from the compilation of numerous bathymetric surveys made available by providers of 24 European countries, and include satellite derived bathymetry information derived from Landsat 8 imagery. Despite a general harmonization of the EMODnet data, this still has variable coverage densities associated with the data collection and survey resources[19]. This work used the XYZ data version of the EMODnet F3 DTM tile, 2018 version[23], set using the WGS84 projection system (EPSG:4326) and with a general1/16X1/16 arc minutes grid, which at this latitude is approximately 115.6 m x 115.6 m. The XYZ data were loaded in the GIS software to produce DEM bathymetry raster and slope map rasters. These maps were reprojected using the WGS 84 UTM29N coordinate system (EPSG: 32629), upon which all the mapping and measurements were made. This is also the default projection system of the data provided. This is also the default projection system of the data provided in the repository[24].

Landslide morphometric mapping

Mapping of the landslide morphological features observed on the DEMs was made using 2D and 3D visualisation perspectives on GIS software to delimit the scars and limits. Landslide morphometric mapping followed, as possible, established criteria[1] for direct measurement features (Figure 3), complemented by additional calculated parameters. Each landslides feature was identified with a unique reference ID (identified as Scar_ID) to which all morphometric parameters were associated. Individualised shapefiles were produced, namely: point features to identify the location of each slide; line features for the scar limit, and landslide length and width; and polygon features to delimit the landslide perimeter. The initial association process between these shapefiles was based on an automated proximity detection between the features. The final merged shapefile was examined for consistency and the correct match between the different elements. The inaccurate records were edited and the shapefiles re-associated. After the manual interpretation on the features on the DEM, automated processes were used to calculate additional parameters to populate the database. The parameter list and description are provided in Table 1. In the instances where it was possible to delineate the deposit associated to the landslide, this was delineated based on the morphological character displayed on the bathymetry DEM. A second set of parameters was mapped for the deposit length, width and perimeter and area. The equivalent parameters were determined for the landslide evacuation region by subtracting the value of the deposit parameters from the total measurements.

Volume calculation

For volume calculation, a DEM raster was calculated to represent the pre-landslide morphology (Figure 2). To produce this surface, we created a copy of the bathymetry raster and clipped it using the landslide limits to remove the data within the polygon. For the following step the gaps were filled using a multilevel b-spline interpolation, further resampled to a 50 x 50 grid. The low-frequency raster component derived from this calculation was used as the model for pre-landslide morphology. The landslide evacuation volume was then calculated using the QGis Volume Calculation Tool plugin, where the bathymetry and pre-failure DEMs were used as base and top surfaces, respectively. This tool allows the assignment of a polygon to delimit the area of operation, thus allowing a constrained volume calculation within each individual landslide limit and the immediate addition of the value to the corresponding Scar_ID in the attribute table. This greatly optimised the volume calculation procedure for all occurrences. The volume calculation used the fill-and-spill calculation. We kept the values representative of the evacuated volume within the landslide, and discarded any calculated deposit volumes as these cannot be reliable without subsurface data to map the base of the deposit.

Data preparation and visualisation

The final data was compiled in a spreadsheet (MagicLand-Data.xlsx) using the Scar_ID as the merging attribute. Sequential gaps in order of this attribute are due to the manual removal of faulty entries either with erroneous parameters or outside of the target area. These would ultimately skew any statistical analysis based on the dataset. Preliminary data plotting was made using the boxplot functions in R Studio for eight representative morphometric parameters (Figure 4). Logarithmic Y scales were used, and are recommended, for a better visualisation of parameters with very large ranges.

Data Records

The MAGICLAND dataset, available through the Open Science Framework (www.doi.org/ 10.17605/OSF.IO/S96RW), includes a set of files with the landslide shapefiles, relevant maps in GeoTIFF format, and data records Microsoft Excel spreadsheets. Table 1, describing the morphometric parameters analysed, is also included as in the dataset (MagicLand-Parameters.xlsx). The main data spreadsheet (MagicLand-Data.xlsx) includes the 1552 data entries and parameters. A subset corresponding to the morphometric properties of the deposit and evacuation regions is on a separate file data (MagicLand-DepositLS.xlsx). The shapefiles relative to the landslide location points, scars and areas are included in the respective zip files. The base bathymetry DEM (MagicLand-BathymetryXYZ.tiff), slope map (MagicLand-slopemap.tiff), reconstructed pre-landslide DEM (BathymReconstruct-Resample50x50_LowPassFilter.tiff) and the cover surface clipped to the landslide area (MagicLand-ReconstCover.tiff) are included.

Technical Validation

The dataset presented exhibits sources of uncertainty inherent to distinct steps of the data compilation. These can be attributed to the base dataset used, to the manual interpretation of landslide scars, perimeter, length and width, and from measurement accuracy.

DEM resolution

The measurements derived from the DEM have an inherent data uncertainty derived from its resolution. Exact details are not provided as the EMODnet data derives from the compilation of multiple surveys. This may increase inaccuracies and artifacts, a common issue with bathymetric data[25]. As the dataset used has an harmonised resolution of 115.6 m x 115.6 m, features smaller than these values were not identified. The lower resolution areas of DEMs can also compromise the calculated slope values[26] as no detailed morphologies are represented. On our dataset this issue has implications for the mapping and measurement of landslide parameters, particularly towards the western and southwestern limits (Figure 1). Here, the poorer data resolution is perceptible from the smoothed, less detailed contour lines. Consequently, a lower number of landslides were mapped toward the western limits of the DEM.

Interpreter bias and data limitations

The manual interpretation of the landslide consists in digitising lines and polygons close to the perceived morphological limits, prone to variations between different individuals and can be influenced by factors such as map resolution and visualisation scale. While major parameters such as length or height tend to lead to low variability, others such as width or the delimitation of the evacuation and deposition areas are prone to higher variability[1]. This is prone to happen during replication of our work, especially for parameters defined as single value landslide features that effectively change along its length. Nevertheless, the high number of samples likely attenuates the interpreter-derived variability and minimises any deviation from the statistical trends obtained (Figure 4). The delimitation of the landslide deposit, when identifiable, is likely underestimated as the DEM only expresses seafloor morphologies. Consequently, when the landslide deposit is partially or fully buried, the deposit and full landslide real length may be higher than the values recorded.

Volume calculation

The accurate volume calculation of the 1552 landslides presented the biggest challenge as we tried to use a uniform method that is applicable to all landslides. Interpolated top surfaces have been successfully used to reconstruct top landslide morphologies[9], and this method is suitable to use in our database. While on longitudinal sections the reconstructed surface has adequate matches with the landslide limits on the bathymetry DEM, transverse sections clipped to the landslide limits may intersect the sidewall at point below its apex. Thus, absolute volume calculation can be underestimated. The reconstruction may also present limitations for smaller landslides in low slope gradient areas. However, this compromise is required to allow the swift volume computation for all elements identified. Furthermore, it should not significantly affect comparative analysis of relative landslide volume magnitude between distinct examples or locations.

Measurement usage in 3D

Line and polygon features representative of quantitative measurements mapped on 2D were projected and recalculated over the 3D DEM in order to mitigate the effect of slope gradients on quantification errors. Figure 5 illustrates the effect of slope gradient on the true length measurement of the morphological features. Very low slope angles will have minimal impact on the length measurements, but for angles of 15 degrees the 2D length can be 20% shorter than the real measurement. Towards the extreme values of our sample, of circa 30 degrees, this effect can lead to a 2D length measurement around 35% shorter than a more realistic measurement. The same principle is valid for width, perimeter and areas measurements. Consequently, our representations of these parameters always accounted for the topography effect. The data table includes both 2D and 3D measurement values (Table 1).

Usage Notes

This section is optional

All researchers interested in submarine geomorphology, landslides and GIS are free to use the datasets provided at will, with appropriate acknowledgement of the source. The data provided in the repository allows an immediate reproducibility of the results and opens possibilities for further statistical analysis and integration with other databases – being that for individual research items or integration at wider scale. The majority of the work was produced using QGIS v3.14, but all items are importable to any GIS software of choice. Despite the high number of features mapped, there are many more occurrences of landslide and mass-movement features passive of being mapped. Further versions of the MAGICLAND database will make efforts to integrate subsurface information and higher detail metrics when higher resolution bathymetric data is available. Researchers are welcome to contribute to the development of this dataset as deemed fit, either by improving knowledge of the mapped features or adding new ones.

Code Availability

No relevant code was produced to prepare or analyse the dataset. The exemption are the simple boxplots for the landslide parameter representation and the scatter plot for the slope effect on length measurement, both produced in R Studio.

Acknowledgements

This work is supported by the project MAGICLAND - MArine Geo-hazards InduCed by underwater LANDslides in the SW Iberian Margin (Ref: PTDC/CTA-GEO/30381/2017), funded by the Fundação para a Ciência e Tecnologia (FCT), Portugal. The authors wish also to acknowledge the financial support of FCT through project UIDB/50019/2020 – IDL.

Author contributions

Davide Gamboa – Developing and conceptualisation of the database; data preparation and loading; data acquisition and mapping; data processing; data visualisation script writing; manuscript concept preparation; manuscript writing and organisation; manuscript editing.

Rachid Omira - Developing and conceptualisation of the database; data review; manuscript revision and editing; funding acquisition.

Pedro Terrinha - Manuscript revision and editing; data support; provision of software and IT equipment.

Competing interests

There are no conflicts of interests.

Figures

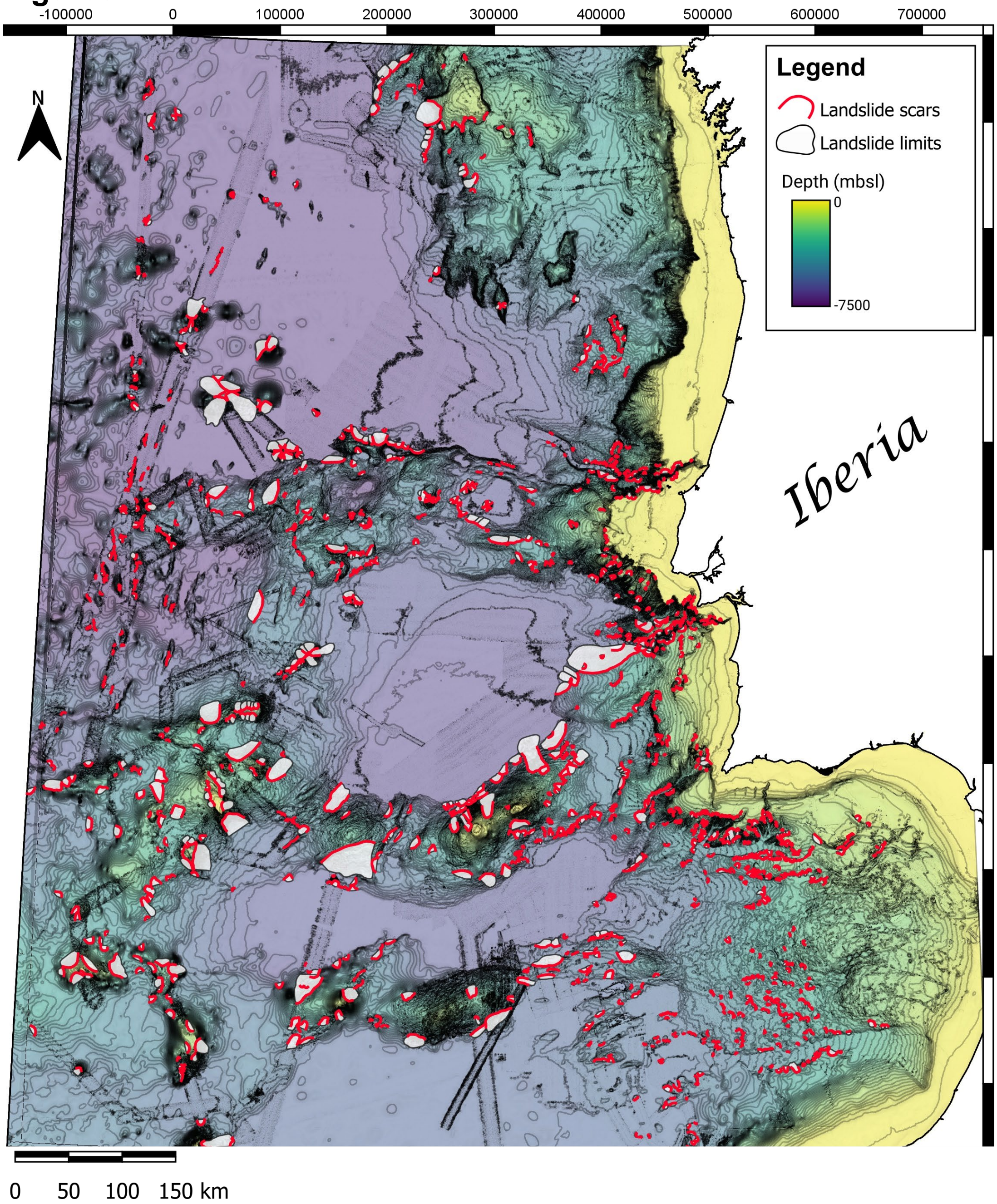

Figure 1

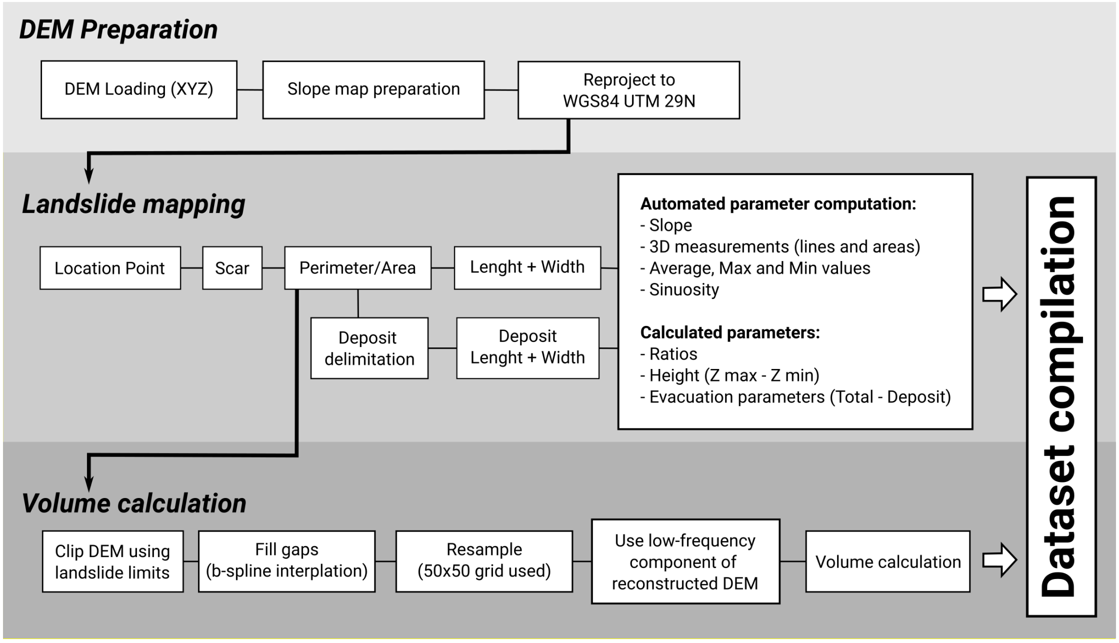

Figure 2

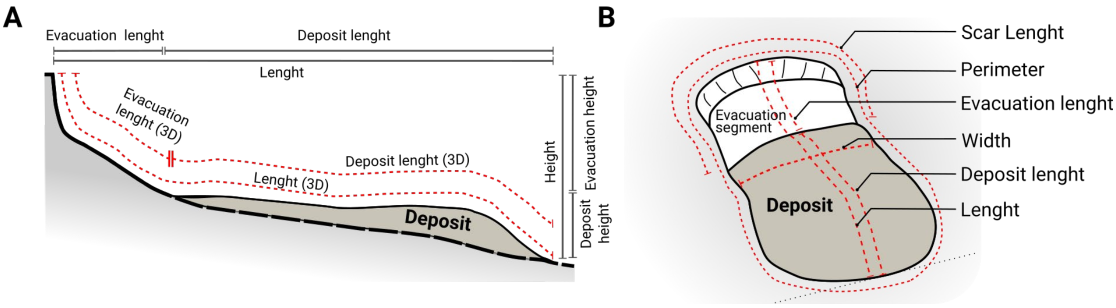

Figure 3

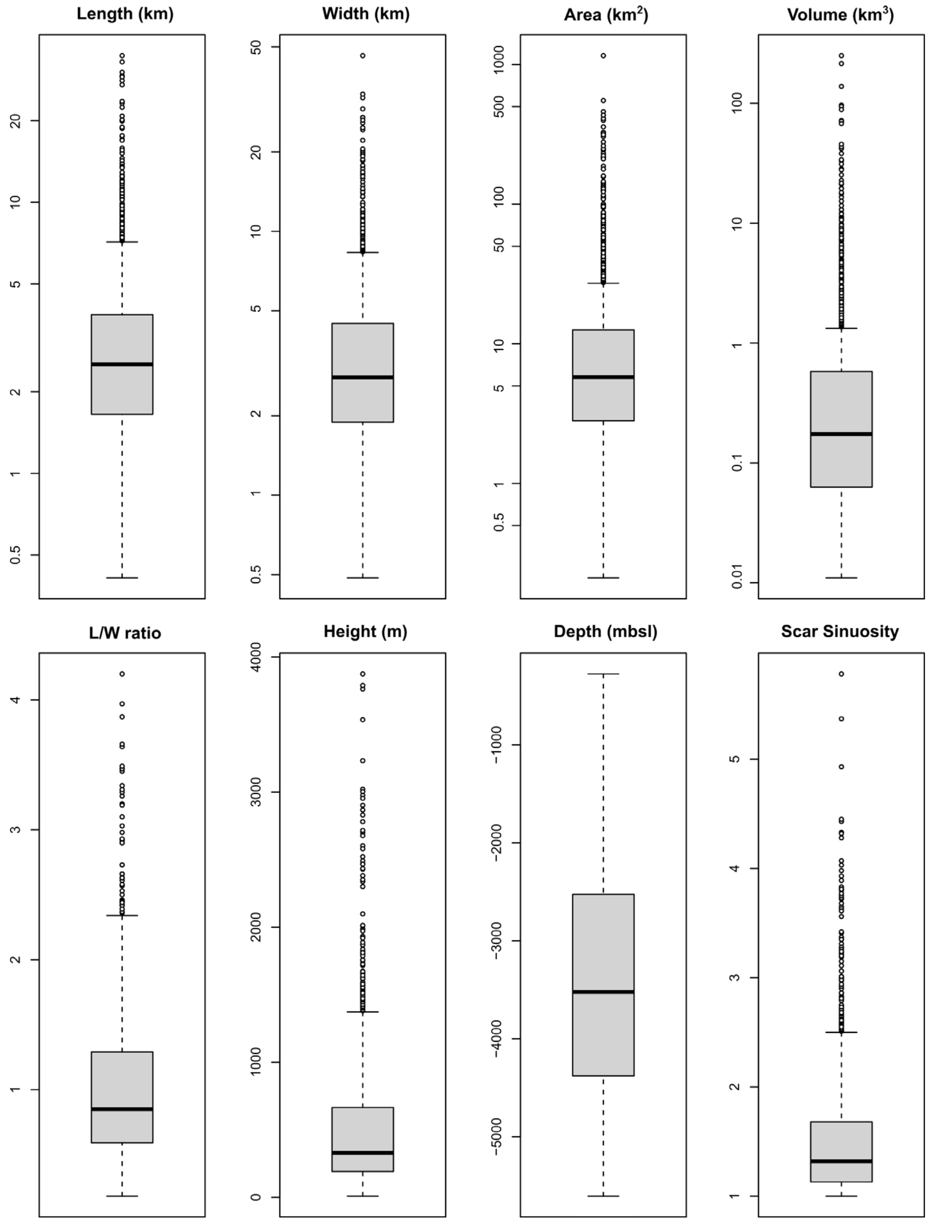

Figure 4

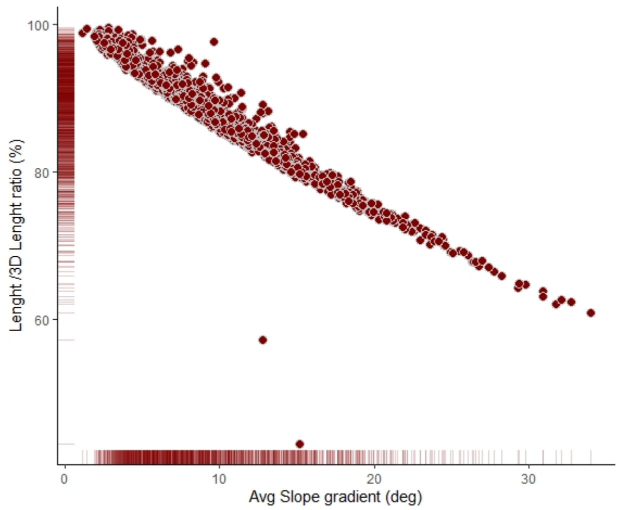

Figure 5

Figure Legends

Figure 1 – Map of the landslides in the study area offshore West and Southwest Iberia. The red lines trace the limit of morphological scars identified on the EMODnet DEM. The grey polygons adjacent to the scars depict the landslide area, but only major ones are discernible at the presented scale. The map is a blend of bathymetric values and calculated slope. Contour lines were calculated from the DEM using a spacing of 100 m.

Figure 2 - Workflow diagram of the landslide mapping and analysis procedure.

Figure 3 - Schematic diagram of analysed landslide parameters. A) Profile view along the landslide limit, including the subdivision between the evacuation and deposit sections. Horizontal length lines at the top are representative of the 2D measurements, while the dashed red lines represent 3D length measurements fitted to the DEM relief. The Height value represents the vertical different between the minimum and maximum depth. B) Perspective diagram to represent the areal morphometric parameters analysed.

Figure 4 – Boxplots summarizing the observations of eight selected parameters. Logarithmic scales were used to represent the y-axis of Length, Width, Area and Volume for a clearer assessment of the distribution ranges.

Figure 5 – Scatter plot representing the impact of slope gradient on the 2D or 3D Length measurement. The Length ratio indicates how much the 2D and 3D measurement differs, with values closer to 100% indicating a minimum or no difference. As shown, the lower the slope gradient, the lower the 2D Length diverges from the real topographic value. The fringes adjacent to the plot axis represent the frequency of registered values.

Tables

Parameter	Description
Scar_ID	Unique identifier of the landslide feature
Confidence	Confidence of the landslide mapping quality - classified as 1,2 or 3.
MultiScar	Y= mapped scar item includes coalesced scar; N= only a single scar is mapped
X	X position of the landslide data point in decimal degrees
Y	Y position of the landslide data point in decimal degrees
Z	Reference depth value of the landslide
L (km)	Length mapped on the raster as 2D vector
L3D (km)	Length value derived from the projection of the vector on the 3D surface
L ratio	Ratio between the L3D and L parameters
W (km)	Width mapped on the raster as 2D vector
W3D (km)	Width value derived from the projection of the vector on the 3D surface
L/W	Length-Width ratio
L/W 3D (km)	Length-Width ratio calculated using the 3D measurement
H (m)	Height of the landslide, calculated as the different between minimum and maximum Z
H/L	Height-Length ratio
L/H	Length-Height ratio
Perimeter (km)	Perimeter of the landslide-delimiting polygon
Area (km^2)	Area of the landslide calculated within the polygon
Area3D (km^2)	Total surface area of the landslide derived from the 3D DEM
ScarL (km)	Length of the landslide scar
ScarSin	Sinuosity of the line delimiting the landslide scar
ScarAvgElev (m)	Average elevation (depth) of the landslide scar
ScarL3D (km)	Scar length measured along the 3D surface
LZmin (m)	Minimum Z
LZmax (m)	Maximum Z
LAvSlope (deg)	Average slope of the length vector along the landslide remobilisation direction
V (km^3)	Calculated volume remobilised by the landslide
DepositL (km)	Length of the deposit segment in 2D
DepositL3D (km)	Length of the deposit segment in 3D
DepAvgDepth (m)	Average depth of the deposit
DepositAvgSlp (deg)	Average slope of the deposit segment
DepositH (m)	Height of the deposit segment
DepositArea (km^2)	Area of the deposit segment in 2D
DepositA3D (km^2)	Area of the deposit segment in 3D
EvacL (km)	Length of the evacuation segment in 2D
EvacL3D (km)	Length of the evacuation segment in 3D
EvacAvgDepth (m)	Average depth of the evacuation segment
EvacAvgSlope (deg)	Average slope of the evacuation segment
EvacH (m)	Height of the evacuation segment
EvacA3D (km^2)	Area of the evacuation segment in 3D

Table 1 – List of the morphometric parameters used in the MAGICLAND database.

References

1. Clare, M. *et al.* A consistent global approach for the morphometric characterization of subaqueous landslides. in *Subaqueous Mass Movements and Their Consequences: Assessing Geohazards, Environmental Implications and Economic Significance of Subaqueous Landslides* (eds. Lintern, D. G. et al.) vol. 477 455–477 (Geological Society, London, Special Publications 477, 2019).
2. Ward, S. N. & Day, S. Cumbre Vieja volcano—potential collapse and tsunami at La Palma, Canary Islands. *Geophys. Res. Lett.* **28**, 3397–3400 (2001).
3. Omira, R. *et al.* Deep-water seamounts, a potential source of tsunami generated by landslides? The Hirondelle Seamount, NE Atlantic. *Mar. Geol.* **379**, 267–280 (2016).
4. Shipp, C., Nott, J. A. & Newlin, J. A. Physical characteristics and impact of mass transport complexes on deepwater jetted conductors and suction anchor piles. in (2004).
5. De Mol, B., Huvenne, V. & Canals, M. Cold-water coral banks and submarine landslides: a review. *Int. J. Earth Sci.* **98**, 885–899 (2009).
6. Mosher, D. C., Shimeld, J. W., Hutchinson, D. R. & Jackson, H. R. Canadian UNCLOS extended continental shelf program seismic data holdings (2006–2011). *Geol. Surv. Can. Open File* **7938**, (2016).
7. Moscardelli, L. & Wood, L. Morphometry of mass-transport deposits as a predictive tool. *Geol. Soc. Am. Bull.* **128**, 47–80 (2016).
8. Twichell, D. C., Chaytor, J. D., ten Brink, U. S. & Buczkowski, B. Morphology of late Quaternary submarine landslides along the U.S. Atlantic continental margin. *Mar. Geol.* **264**, 4–15 (2009).
9. Chaytor, J. D., ten Brink, U. S., Solow, A. R. & Andrews, B. D. Size distribution of submarine landslides along the U.S. Atlantic margin. *Mar. Geol.* **264**, 16–27 (2009).

10. Urgeles, R. & Camerlenghi, A. Submarine landslides of the Mediterranean Sea: Trigger mechanisms, dynamics, and frequency-magnitude distribution. *J. Geophys. Res. Earth Surf.* **118**, 2600–2618 (2013).
11. León, R. *et al.* Geological and tectonic controls on morphometrics of submarine landslides of the Spanish margins. in *Subaqueous Mass Movements and their Consequences: Advances in Process Understanding, Monitoring and Hazard AssessmentsGeological Society, London, Special Publications* (eds. Georgiopoulou, A. et al.) vol. 500 495–513 (Geological Society, London, Special Publications, 2020).
12. Clarke, S. L., Hubble, T. C., Miao, G., Airey, D. W. & Ward, S. N. Eastern Australia's submarine landslides: implications for tsunami hazard between Jervis Bay and Fraser Island. *Landslides* **16**, 2059–2085 (2019).
13. ten Brink, U. S., Andrews, B. D. & Miller, N. C. Seismicity and sedimentation rate effects on submarine slope stability. *Geology* **44**, 563–566 (2016).
14. Blahůt, J. *et al.* A comprehensive global database of giant landslides on volcanic islands. *Landslides* **16**, 2045–2052 (2019).
15. Terrinha, P. *et al.* Tsunamigenic-seismogenic structures, neotectonics, sedimentary processes and slope instability on the southwest Portuguese Margin. *Mar. Geol.* **195**, 55–73 (2003).
16. Zitellini, N. *et al.* The quest for the Africa–Eurasia plate boundary west of the Strait of Gibraltar. *Earth Planet. Sci. Lett.* **280**, 13–50 (2009).
17. Zitellini, N. *et al.* Source of 1755 Lisbon earthquake and tsunami investigated. *Eos Trans. Am. Geophys. Union* **82**, 285–291 (2001).
18. Collico, S. *et al.* Probabilistic mapping of earthquake-induced submarine landslide susceptibility in the South-West Iberian margin. *Mar. Geol.* **429**, 106296 (2020).
19. Innocenti, C., Battaglini, L., D'Angelo, S. & Fiorentino, A. Submarine landslides: mapping the susceptibility in European seas. *Q. J. Eng. Geol. Hydrogeol.* **54**, (2021).

20. Terrinha, P. *et al.* The Tagus River delta landslide, off Lisbon, Portugal. Implications for Marine geo-hazards. *Mar. Geol.* **416**, 105983 (2019).
21. Gamboa, D. *et al.* Destructive episodes and morphological rejuvenation during the lifecycles of tectonically active seamounts: Insights from the Gorringe Bank in the NE Atlantic. *Earth Planet. Sci. Lett.* **559**, 116772 (2021).
22. Teixeira, M. *et al.* Interaction of alongslope and downslope processes in the Alentejo Margin (SW Iberia)–Implications on slope stability. *Mar. Geol.* **410**, 88–108 (2019).
23. EMODnet Bathymetry Consortium. EMODnet Digital Bathymetry (DTM 2018), EMODnet Bathymetry Consortium. (2018).
24. Gamboa, D. & Omira, R. The MAGICLAND submarine landslide database - offshore WSW Iberia. (2021) doi:10.17605/OSF.IO/S96RW.
25. Kint, L. *et al.* Uncertainty assessment applied to marine subsurface datasets. *Q. J. Eng. Geol. Hydrogeol.* **54**, (2021).
26. Wilson, M. F. J., O'Connell, B., Brown, C., Guinan, J. C. & Grehan, A. J. Multiscale Terrain Analysis of Multibeam Bathymetry Data for Habitat Mapping on the Continental Slope. *Mar. Geod.* **30**, 3–35 (2007).